Relaxation Behavior of Poly(lactic acid)/Poly(butylene succinate) Blend and a New Method for Calculating Its Interfacial Tension

Lin-Qiong Xu, Han-Xiong Huang

Lab for Micro Molding and Polymer Rheology, The Key Laboratory of Polymer Processing Engineering of the Ministry of Education, South China University of Technology, Guangzhou 510640, People's Republic of China

Received 18 March 2011; accepted 23 January 2012
DOI 10.1002/app.36910
Published online in Wiley Online Library (wileyonlinelibrary.com).

ABSTRACT: The biomass-based blend of 80/20 (w/w) poly(lactic acid)/poly(butylene succinate) (PLA/PBS) is prepared using an extruder. The prepared blend shows a typical droplet-matrix morphology. The relaxation behavior of the blend is investigated in terms of storage modulus, loss tangent, and Cole–Cole plots. In the low frequency region, the blend exhibits higher elastic indices than the pure components on the storage modulus and loss tangent curves, and remarkable deviation from a semicircular shape on the Cole–Cole plot. These features are thought to arise from the relaxation of the deformed droplets. The loss tangent curve is more sensitive to the relaxation behavior of the deformed droplets than the storage modulus curve. Moreover, the complex viscosity of the blend is separated into real and imaginary parts to further analyze its relaxation behavior. Three relaxation times for the blend are defined on the curve of the imaginary part of the viscosity. It is demonstrated that the reciprocal of the frequency corresponding to the peak in the low frequency region on the imaginary part curve is equal to the longest relaxation time of the blend obtained from the storage modulus curve. Based on this result, a new method is proposed to calculate the interfacial tension between the PLA and PBS in the blend, which is 3.7 mN/m. © 2012 Wiley Periodicals, Inc. J Appl Polym Sci 000: 000–000, 2012

Key words: biodegradable; blends; morphology; polymer rheology; relaxation

INTRODUCTION

Recently, great attention has been paid to biodegradable aliphatic polyesters, such as poly(lactic acid) (PLA),[1–5] poly(butylene succinate) (PBS),[6–10] poly(ε-caprolactone) (PCL),[11–13] and poly(3-hydroxybutyrate) (PHB),[14,15] because of a rapid growth of intensive interest in the global environment. Especially, the PLA has been used in biological applications because of its good biocompatibility, biodegradability, and various mechanical properties (such as high rigidity).[16–18] However, its brittleness is a major defect for many applications. In order to improve its toughness, the blends of the PLA with other flexible and biodegradable aliphatic polyesters, such as PBS[6–10] and PCL,[11–13] have been investigated. For example, Shibata et al.[6] reported that the poly(L-lactide) (PLLA)/PBS blends show higher elongation at break than pure PLLA. However, PLA and PBS are immiscible in the molten state and their blends exhibit phase-separated structure.[9] Interfacial properties between the components in the immiscible blends play an important role in their phase morphology and mechanical properties.

The relaxation behavior of the blends may give useful information on their interfacial properties. For instance, the stronger the interfacial adhesion is, the longer time the relaxation of the deformed droplets takes up. The dynamic rheological functions, such as the Cole–Cole, storage moduli, and loss tangent plots, can reflect the relaxation behavior of the blends. On the Cole–Cole plot, any deviation from a smooth and semicircular shape indicates the appearance of the second relaxation mechanism.[19,20] The loss tangent curve was also used to analyze the relaxation behavior for the immiscible blends by some researchers. For example, Peon et al.[21] reported that this curve reveals the relaxation mechanism of the ethylene/vinyl acetate copolymer and metallocene-catalyzed linear polyethylene (EVAc/mPE) blends. Palierne[22] proposed a constitutive equation for the complex modulus as a function of the volume fraction and volume average radius of the dispersed droplets and the interfacial tension and viscosity ratio of the two components for the blend with a droplet-matrix morphology. On the assumption that the droplet size distribution is narrow and the interfacial tension is independent of the local shear and the variation of interfacial

Correspondence to: H.-X. Huang (mmhuang@scut.edu.cn).
Contract grant sponsor: National Natural Science Foundation of China; contract grant number: 20874031, 11172105.
Contract grant sponsor: Guangdong Provincial Natural Science Foundation; contract grant number: S2011010002085.

area, Graebling et al.[23] simplified the Palierne model. Moreover, for a blend of two viscoelastic fluids, Graebling et al.[23] defined several parameters associated with the morphology of the blend, namely, λ_M, λ_P, λ_D, and G_P. Among them, λ_M is the mean relaxation time of the blend, λ_P is the time corresponding to the beginning of the droplet deformation, λ_D is the longest relaxation time of the blend and corresponds to the total shape relaxation of the droplets, and G_P is the modulus corresponding to the secondary characteristic plateau. These parameters can be calculated using the following equations:

$$\lambda_D = \frac{R_V \eta_{0,m}}{4\alpha} \frac{(19K+16)[2K+3-2\phi(K-1)]}{10(K+1)-2\phi(5K+2)} \quad (1)$$

$$\lambda_P^2 = \frac{\eta_{0,m}\lambda_m}{G_P}\left\{\frac{3(1-\phi)(1-\chi)}{2K+3-2\phi(K-1)} + \frac{[2K+3+3\phi(K-1)][2K+3\chi-2\phi(K-\chi)]}{[2K+3-2\phi(K-1)]^2}\right\} \quad (2)$$

$$\lambda_M^2 = \lambda_m^2\left[\frac{3(1-\phi)(1-\chi)}{2K+3+3\phi(K-1)} + \frac{2K+3\chi-2\phi(K-\chi)}{2K+3-2\phi(K-1)}\right] \quad (3)$$

$$G_P = 20\frac{\alpha}{R_V}\frac{\phi}{[2K+3-2\phi(K-1)]^2} \quad (4)$$

where $K = \eta_{0,i}/\eta_{0,m}$ is the zero-shear viscosity ratio and $\chi = \lambda_i/\lambda_m$ is the relaxation time ratio of the dispersed phase and matrix; α is the interfacial tension between the components of the blend; ϕ is the volume fraction of the dispersed phase; R_V is the volume average radius of the dispersed droplets.

The Palierne model can be used to determine the interfacial tension between the two components in the blend using rheological data if the volume average radius of the dispersed droplets is available.[9,13,24] However, this method is based on the adjustment of the interfacial tension for the Palierne model to fit the experimental data in the tested frequency region, which would lead to a large variation of the results.[24] Moreover, this method would be invalid for some blends, such as poly(methyl methacrylate)/polypropylene blends.[24] In addition to this method, some researchers obtained the longest relaxation time of the blend from the weight relaxation spectrum of blend and then used eq. (1) to calculate the interfacial tension.[13,24,25] However, the continuous relaxation spectrum, which is an important component of the weight relaxation spectrum, is difficult to be obtained.[26]

In this work, the PLA/PBS blend is prepared using a modular single-screw extruder (SSE) with special screw elements. The relaxation behavior of the prepared PLA/PBS blend is investigated in terms of storage modulus, loss tangent, and Cole–Cole plots. Moreover, the complex viscosity of the blend is separated into the real and imaginary parts, and then three relaxation times are defined on the imaginary one. A new method is proposed to calculate the interfacial tension between the two components in the PLA/PBS blend by analyzing its relaxation behavior, which is reflected on the curve of the imaginary part of the complex viscosity.

EXPERIMENTAL

Materials and equipment

As the matrix phase, the PLA (grade 2002D, NatureWorks® LLC, Minnetonka, Minnesota) has a melt flow index of 8.8 g/10 min (210°C, 2.16 kg) and density of 1.24 g/cm^3. PBS (1903I, Hangzhou Xinfu Pharmaceutical, Zhejiang, China) with a melt-flow index of 15.3 g/10 min (150°C, 2.16 kg) and a density of 1.24 g/cm^3 was used as the dispersed phase. The weight ratio of PLA and PBS was 80/20.

Although the conventional SSE has poor mixing performance compared with the twin-screw extruder, SSE with special screw elements can provide good mixing under lower shear intensity,[27–29] which is favorable to the processing of the biodegradable polyesters. In the present work, the blend was prepared by a modular SSE with a screw diameter of 45 mm and a length-to-diameter ratio of 30 : 1. The extruder screw with special screw elements was used to provide good mixing.

Sample preparation

PLA and PBS were dried at 90°C for 2 h and 60°C for 4 h in a vacuum oven, respectively. Then PLA and PBS were blended in the SSE. The extruder was operated at temperature profiles of 160–180–180–180°C from the feeding zone to the die. The feeding rate and screw speed were set at 3 kg/h and 40 rpm, respectively. For comparison, the pure PLA and PBS were also processed under the same conditions. The samples for scanning electron microscope (SEM) observation and dynamic rheological measurement were collected from the exit of the extruder and quenched in iced water as soon as possible to preserve the blend morphology. Then, all samples were dried at 60°C for 4 h in a vacuum oven.

Characterization

Bohlin Gemini 200 Rheometer (Bohlin Ltd., Worcestershire, UK) equipped with a parallel-plate fixture (25 mm diameter) was used in an oscillatory mode to conduct dynamic frequency sweep tests. The complex viscosity (η^*), storage moduli (G'), and loss moduli (G'') as a function of angular frequency (ω) ranging from 0.0628 to 628 rad/s were measured at 180°C. A fixed strain of 5% was used to ensure that

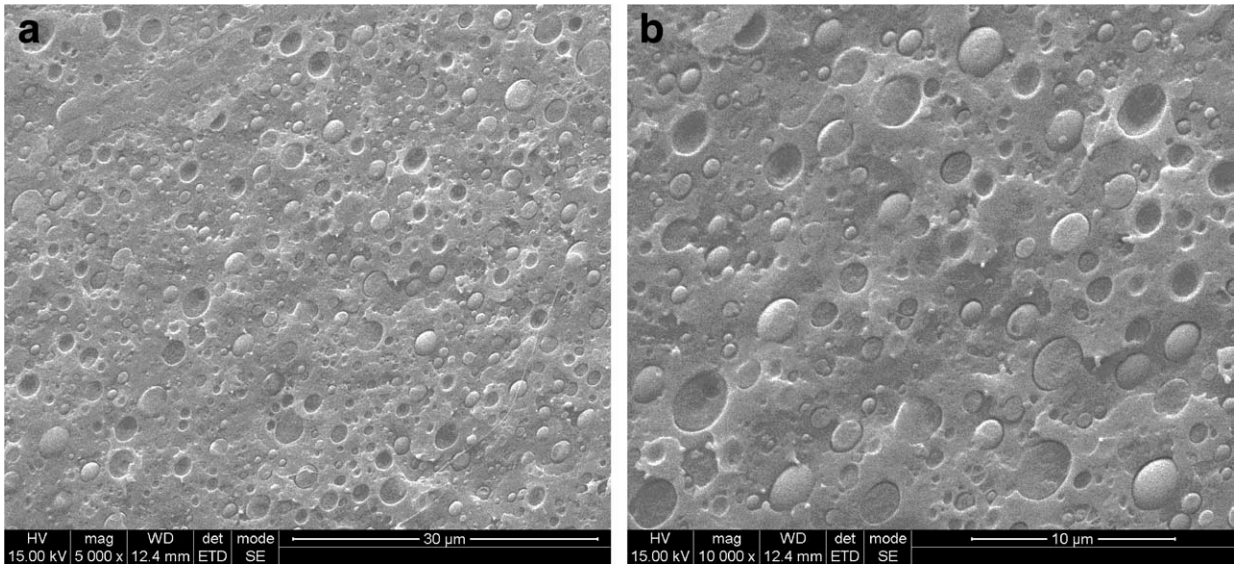

Figure 1 SEM micrographs with (a) lower and (b) higher magnifications for prepared PLA/PBS blend.

the measurements were carried out within the linear viscoelastic range of the samples investigated.

The collected blend sample was fractured in its middle along the melt-flow direction in liquid nitrogen and then sputter coated with gold. The observation of the phase morphology was conducted on the cryo-fractured surface using SEM (Quanta 200, FEI, Eindhoven, Holland). The diameters of the dispersed droplets were measured using Image Pro image analysis software (Media Cybernetics Inc., Silver Spring, Maryland). The mean diameter of a single droplet was calculated by averaging all of the diameters obtained from a rotation of 5° one time with the droplet centroid as the center. The volume and number average radii (R_V, R_n) of the dispersed droplets were estimated by:

$$R_V = \frac{\sum_i n_i R_i^4}{\sum_i n_i R_i^3} \quad (5)$$

$$R_n = \frac{\sum_i n_i R_i}{\sum_i n_i} \quad (6)$$

where R_i is the radius of each droplet and n_i is the number of droplets with R_i.

RESULTS AND DISCUSSION

Phase morphology

Figure 1 illustrates the SEM micrographs on the cryo-fractured surface for the prepared PLA/PBS blend. As expected, phase separation occurs in the blend. The spherical PBS droplets with smooth surface and nonuniform size distribution are distributed in the PLA phase. The R_V and R_n of the dispersed droplets calculated by eqs. (5) and (6) are 0.65 and 0.32 µm, respectively.

Complex viscosity

Figure 2 shows the η* versus ω curves for the PLA/PBS blend as well as the pure components at 180°C. It is observed that the η*(ω) curve for the blend is located between those of the pure PLA and PBS within tested frequency region. Moreover, the blend begins to exhibit the shear thinning behavior at a frequency lower than those for the neat components. This phenomenon may be attributed to the relaxation of the deformed droplets and interfacial slip between two phases and was also observed for other blends, such as PLA/poly(-butylenes adipate-*co*-terephthalate)[5] and EVAc/mPE[21] blends.

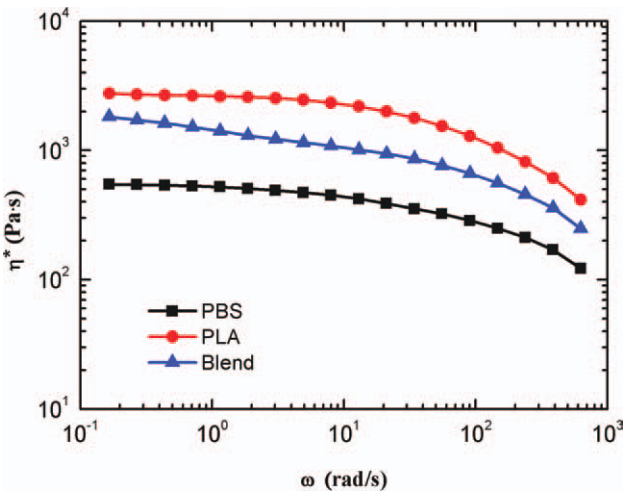

Figure 2 Complex viscosity versus angle frequency for PLA/PBS blend and pure PLA and PBS. [Color figure can be viewed in the online issue, which is available at wileyonlinelibrary.com.]

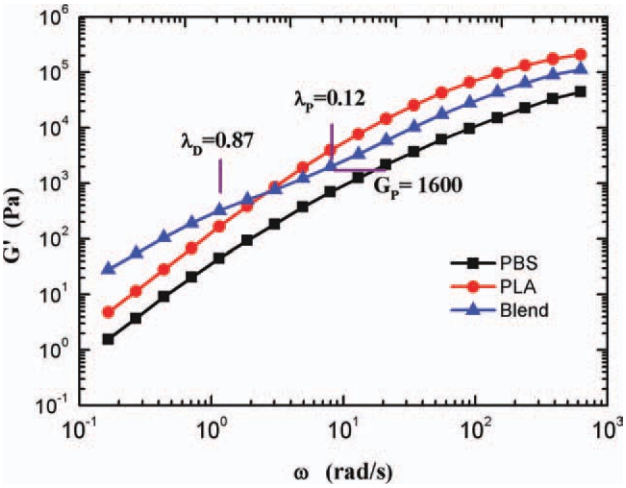

Figure 3 Storage modulus versus angle frequency for PLA/PBS blend and pure PLA and PBS. [Color figure can be viewed in the online issue, which is available at wileyonlinelibrary.com.]

Relaxation behavior

As mentioned in the Introduction section, the Cole–Cole, storage moduli, and loss tangent plots can reflect the relaxation behavior of the blends. In this work, these three dynamic rheological functions were used to analyze the relaxation behavior of the prepared PLA/PBS blend. Figure 3 exhibits the G' versus ω curves of the PLA/PBS blend along with the pure components. It can be clearly seen that the $G'(\omega)$ curve of the blend is located between those of pure PLA and PBS in the high frequency region, whereas the value of $G'(\omega)$ of the blend is larger than those of both pure components in the low frequency region. Loss tangent ($\tan\delta = G''/G'$) values of the PLA/PBS blend and pure components were calculated and the results are displayed in Figure 4. As can be seen that the tanδ of the blend is located between those of the pure components in the high frequency region. However, the tanδ of the blend becomes smaller than the values of the pure components when ω is less than 7.98 rad/s.

For the immiscible blends, the enhanced elastic indices exhibiting on the storage modulus and loss tangent curves in both low- and intermediate-frequency regions can be contributed to the shape relaxation of the dispersed droplets during oscillatory shear flow.[21,30] In the high frequency region, the dispersed droplets have no enough time to relax, and the energy supplied by deformation is completely dissipated in the bulk of the matrix. Therefore, the $G'(\omega)$ curve of the blend lies between those of the pure components in the high frequency region.[30]

According to the definitions of the λ_D, λ_P, and G_P mentioned in the Introduction section for the immiscible blends, the approximate values of these three parameters can be directly obtained from $G'(\omega)$ curve and the results are shown in Figure 3. The obtained values of λ_D and λ_P were also displayed on the tanδ curve shown in Figure 4. From Figure 4 it can be seen that these two values just correspond to the turning points on the tanδ curve for the blend. Moreover, comparing Figure 3 with Figure 4 reveals that the plateau on the tanδ curve is more obvious than the secondary plateau on the $G'(\omega)$ curve for the blend, which indicates that the tanδ curve is more sensitive to the relaxation behavior of the deformed droplets than the $G'(\omega)$ curve.

Figure 5 displays the Cole–Cole plots (that is η'' versus η' curves, where $\eta'' = G'/\omega$ and $\eta' = G''/\omega$) of the prepared PLA/PBS blend and pure components. As can be seen, two circular arcs appear on the Cole–Cole plot for the blend, which indicates that a second relaxation mechanism appears.

Now the relaxation behavior of the prepared PLA/PBS blend is further analyzed by plotting its η' and η'' as a function of ω. The results are illustrated in Figure 6, in which the $\eta'(\omega)$ and $\eta''(\omega)$ curves of both pure components are also given. It is observed that the $\eta'(\omega)$ curves look similar to $\eta^*(\omega)$ curves shown in Figure 2 for the PLA/PBS blend and pure PLA and PBS. The $\eta''(\omega)$ curve of the PLA/PBS blend has two peaks, whereas the $\eta''(\omega)$ curves of pure PLA and PBS have only one peak. For the $\eta''(\omega)$ curve of the blend, the reciprocals of the frequencies corresponding to the peak in the high frequency region, to the depression, and to the peak in the low frequency region are defined as the relaxation times of the blend, and denoted as λ_1, $\lambda_{depression}$, and λ_2, respectively. As can be seen in Figure 6, the value of $\eta''(\omega)$ of the blend increases as the ω decreases in two frequency ranges, the one with frequencies higher than $1/\lambda_1$ and the other with frequencies from $1/\lambda_2$ to $1/\lambda_{depression}$. The phenomena in these two frequency ranges are attributed to the relaxation of the blend and

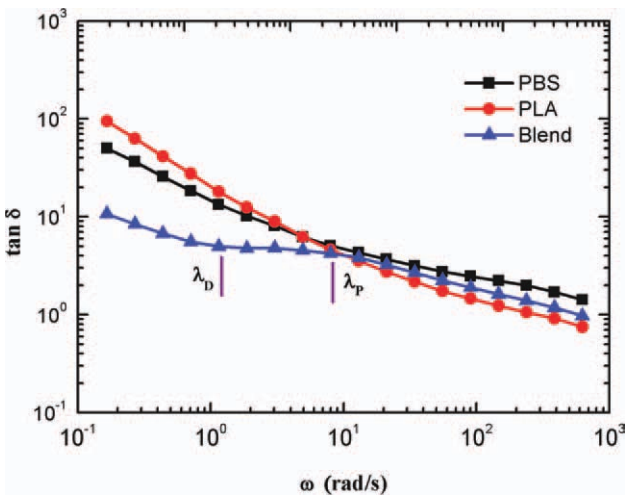

Figure 4 Loss tangent versus angle frequency for PLA/PBS blend and pure PLA and PBS. [Color figure can be viewed in the online issue, which is available at wileyonlinelibrary.com.]

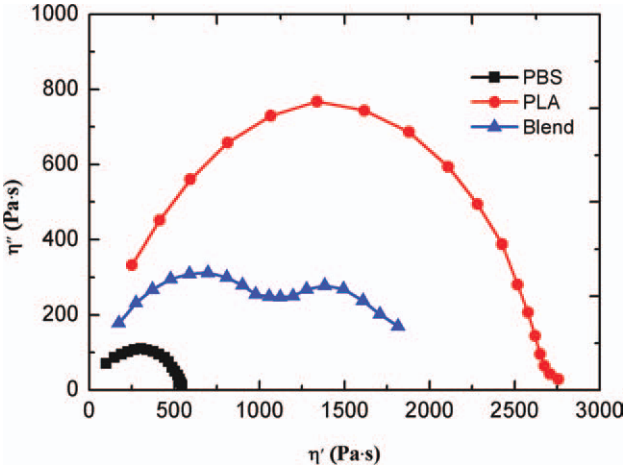

Figure 5 Cole–Cole plots of PLA/PBS blend and pure PLA and PBS. [Color figure can be viewed in the online issue, which is available at wileyonlinelibrary.com.]

the relaxation of deformed droplets, respectively. The value of $\eta''(\omega)$ decreases as ω decreases when ω is less than $1/\lambda_2$, which may be attributed to the complete relaxation of the deformed droplets. Therefore, λ_1, $\lambda_{depression}$, and λ_2 can be regarded as the times corresponding to the relaxation of the blend, beginning of relaxation of the deformed droplets, and total shape relaxation of the droplets, respectively. These three relaxation times as well as the λ_D, λ_P, and G_P obtained from the $G'(\omega)$ curve shown in Figure 3 are listed in Table I. It can be clearly seen that the λ_2 is equal to the λ_D, and the $\lambda_{depression}$ is close to the λ_P.

A new method for calculating the interfacial tension

As mentioned above, the λ_2 obtained from the $\eta''(\omega)$ curve and λ_D obtained from the $G'(\omega)$ curve for the prepared PLA/PBS blend have the same value. In fact, the λ_2 and λ_D are both related to the total shape relaxation of the droplets and have the same physical significance. Therefore, the interfacial tension between the two phases of the PLA/PBS blend is calculated using eq. (1) by substituting the λ_2 obtained from the $\eta''(\omega)$ curve for the λ_D defined on the $G'(\omega)$ curve. In the calculation of the interfacial tension, R_V, $\eta_{0,m}$, and $\eta_{0,i}$ should be used. Using the values of the R_V and R_n of the dispersed PBS droplets given in the Morphology section, the R_V/R_n is calculated, which is equal to 2.0. This meets the condition for the application of the Palierne model, that is, the polydispersity does not exceed a value of about 2.3. The $\eta_{0,m}$, and $\eta_{0,i}$ are calculated by[31]:

$$\eta_0 = \lim_{\omega \to 0} \frac{G''}{\omega} \tag{7}$$

The calculated value of the interfacial tension between the PLA and PBS is 3.7 mN/m, which is close to the value (3.5 mN/m) reported by Yokohara and Yamaguchi, who adjusted the interfacial tension for the Palierne model to fit the experimental data of the PLA/PBS blends in the tested frequency region.[9]

As stated above, the interfacial tension between two phases can be calculated using eq. (1) by substituting the λ_2 obtained from the $\eta''(\omega)$ curve for the λ_D defined on the $G'(\omega)$ curve when the $1/\lambda_D$ is within the tested frequency region. This new method can avoid a large variation of the results by adjusting the interfacial tension for the Palierne model to fit the experimental data at tested frequency region.[24]

Using the previously calculated value of the interfacial tension between the PLA and PBS, the λ_P, λ_M, and G_P are calculated by eqs. (2–4). The λ_m and λ_i are calculated by[31]:

$$\lambda = \lim_{\omega \to 0} \frac{G'}{\omega G''} \tag{8}$$

The calculated values of λ_P, λ_M, and G_P are listed in Table II. Comparing Table I with Table II shows that the calculated values of the λ_P and G_P are close

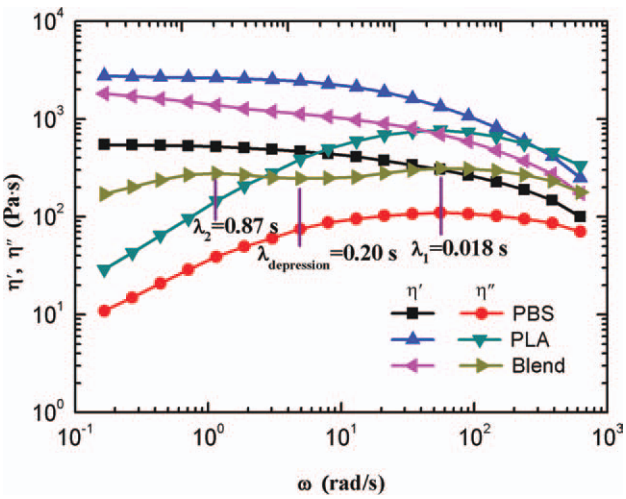

Figure 6 Real and imaginary parts of complex viscosity versus angle frequency for PLA/PBS blend and pure PLA and PBS. [Color figure can be viewed in the online issue, which is available at wileyonlinelibrary.com.]

TABLE I
Relaxation Times Obtained from $\eta''(\omega)$ and $G'(\omega)$ Curves and Secondary Plateau Modulus Obtained from $G'(\omega)$ Curve for PLA/PBS Blend

λ_1 (s)	$\lambda_{depression}$ (s)	λ_2 (s)	λ_P (s)	λ_D (s)	G_P (Pa)
0.018	0.20	0.87	0.12	0.87	1600

TABLE II
Relaxation Times and Secondary Plateau Modulus of PLA/PBS Blend Calculated by Substituting λ_2 for λ_D

λ_P (s)	λ_M (s)	G_P (Pa)
0.16	0.018	1681

to the values obtained from the $G'(\omega)$ curve and the λ_M is equal to λ_1 obtained from the $\eta''(\omega)$ curve. Therefore, it is believed that the aforementioned definition about the three relaxation times for the prepared PLA/PBS blend on its $\eta''(\omega)$ curve and the proposed method for calculating the interfacial tension between two phases are reasonable.

CONCLUSIONS

The dynamic frequency sweep tests showed that the prepared PLA/PBS (80/20, w/w) blend began to exhibit shear thinning behavior at a frequency lower than those for neat components, which was strongly related to the relaxation of the deformed droplets. In addition, the relaxation resulted in the deviation of the curves of the storage modulus, loss tangent, Cole–Cole, and imaginary part of the complex viscosity for the blend from both of the pure components in the low frequency region. Two relaxation times related to the deformed droplets were directly obtained from the storage modulus curve, which just corresponded to the turning points on the loss tangent curve. The reciprocals of the frequencies corresponding to the depression and two peaks on the imaginary part curve of the complex viscosity were regarded as the relaxation times of the blend by analyzing its relaxation behavior being reflected on the curve. Therefore, the interfacial tension between the components of the blend was calculated using an equation derived from the Palierne model with the longest relaxation time of the blend, which was obtained from the imaginary part curve of the complex viscosity. The calculated interfacial tension between the PLA and PBS was 3.7 mN/m. Using the calculated value of the interfacial tension, the relaxation times and secondary plateau modulus of the blend were calculated by equations derived from the Palierne model. The calculated relaxation times and secondary plateau modulus were close to the ones obtained from the rheological curves. So the definitions about the three relaxation times for the prepared PLA/PBS blend on the imaginary part of its complex viscosity and the proposed method for calculating the interfacial tension between two phases were reasonable.

References

1. Arvanitoyannis, I.; Nakayama, A.; Kawasaki, N.; Yamamoto, N. Polymer 1995, 36, 2271.
2. Arvanitoyannis, I. J Macromol Sci Rev Macromol Chem Phys 1999, C39, 205.
3. Nampoothiri, K. M.; Nair, N. R.; John, R. P. Bioresource Technol 2010, 101, 8493.
4. Han, J. J.; Huang, H. X. J Appl Polym Sci 2011, 120, 3217.
5. Li, K.; Peng, J.; Turng, L. S.; Huang, H. X. Adv Polym Technol 2011, 30, 150.
6. Shibata, M.; Inoue, Y.; Miyoshi, M. Polymer 2006, 47, 3557.
7. Harada, M.; Ohya, T.; Iida, K.; Hayashi, H.; Hirano, K.; Fukudal, H. J Appl Polym Sci 2007, 106, 1813.
8. Shibata, M.; Teramoto, N.; Inoue, Y. Polymer 2007, 48, 2768.
9. Yokohara, T.; Yamaguchi, M. Eur Polym J 2008, 44, 677.
10. Yokohara, T.; Okamoto, K.; Yamaguchi, M. J Appl Polym Sci 2010, 117, 2226.
11. Wu, D. F.; Zhang, Y. S.; Zhang, M.; Zhou, W. D. Eur Polym J 2008, 44, 2171.
12. Simoes, C. L.; Viana, J. C.; Cunha, A. M. J Appl Polym Sci 2009, 112, 345.
13. Wu, D. F.; Zhang, Y. S.; Yuan, L. J.; Zhang, M.; Zhou, W. D. J Polym Sci Polym Phys 2010, 48, 756.
14. Ohkoshi, I.; Abe, H.; Doi, Y. Polymer 2000, 41, 5985.
15. Zhang, M.; Thomas, N. L. Adv Polym Technol 2011, 30, 67.
16. Pilla, S.; Kramschuster, A.; Yang, L. Q.; Lee, J.; Gong, S. Q.; Turng, L. S. Mater Sci Eng C 2009, 29, 1258.
17. Kramschuster, A.; Turng, L. S. J Biomed Mater Res B 2010, 92, 366.
18. Armentano, I.; Dottori, M.; Fortunati, E.; Mattioli, S.; Kenny, J. M. Polym Degrad Stab 2010, 95, 2126.
19. Chopra, D.; Kontopoulou, M.; Vlassopoulos, D.; Hatzikiriakos, S. G. Rheol Acta 2002, 41, 10.
20. Li, R. M.; Yu, W.; Zhou, C. X. Polym Bull 2006, 56, 455.
21. Peon, J.; Vega, J. F.; Del Amo, B.; Martinez-Salazar, J. Polymer 2003, 44, 2911.
22. Palierne, J. F. Rheol Acta 1990, 29, 204.
23. Graebling, D.; Muller, R.; Palierne, J. F. Macromolecules 1993, 26, 320.
24. Calvao, P. S.; Yee, M.; Demarquette, N. R. Polymer 2005, 46, 2610.
25. Souza, A. M. C.; Demarquette, N. R. Polymer 2002, 43, 1313.
26. Stadler, F. J.; Bailly, C. Rheol Acta 2009, 48, 33.
27. Huang, H. X.; Huang, Y. F.; Li, X. J. Polym Test 2007, 26, 770.
28. Huang, H. X.; Jiang, G.; Li, X. J. Int Polym Proc 2008, 23, 47.
29. Li, K.; Huang, H. X.; Jiang, G. Polym-Plast Technol Eng 2009, 48, 989.
30. Bousmina, M. Rheol Acta 1999, 38, 251.
31. Ferry, J. D. Viscoelastic Properties of Polymers, 3rd ed.; Wiley: New York, 1980.